Dendrochronologia 65 (2021) 125799

Contents lists available at ScienceDirect

Dendrochronologia

journal homepage: www.elsevier.com/locate/dendro

Ring widths of Rhododendron shrubs reveal a persistent winter warming in the central Himalaya

Shankar Panthi [a,b], Ze-Xin Fan [a,b,c,*], Achim Bräuning [d]

[a] CAS Key Laboratory of Tropical Forest Ecology, Xishuangbanna Tropical Botanical Garden, Chinese Academy of Sciences, Menglun, Mengla, Yunnan 666303, China
[b] Center for Plant Ecology, Core Botanical Gardens, Chinese Academy of Sciences, Xishuangbanna, 666303, China
[c] Ailaoshan Station of Subtropical Forest Ecosystem Studies, Xishuangbanna Tropical Botanical Garden, Chinese Academy of Sciences, Jingdong, Yunnan 676209, China
[d] Institute of Geography, University of Erlangen-Nürnberg, Erlangen 91058, Germany

ARTICLE INFO

Keywords:
Central Himalaya
Climate change
Dendroclimatology
Rhododendron campanulatum
Shrub rings
Winter temperature

ABSTRACT

Himalayan Mountains provide unique opportunities for the extension of shrub-ring based dendroclimatology beyond the upper tree limit. However, little is known about limiting climate factors of shrub growth under harsh environmental conditions. We established a new ring-width chronology of a Himalayan shrub rhododendron (*Rhododendron campanulatum* D. Don) at the upper Krummholz treeline in the Mt. Gaurishankar massif, central Himalaya, Nepal. Bootstrapped correlation analysis showed positive relationships between radial growth and temperatures of all months from previous November to current October. Correlations were the highest with winter (December-February) minimum temperature ($r = 0.781$, $p < 0.001$), indicating that radial growth of *R. campanulatum* is strongly sensitive to winter minimum temperature. The linear regression model explained 61 % of the actual winter minimum temperature variance during the calibration period 1960–2013. Periods of low and high minimum winter temperatures in the central Himalaya were consistent with cool and warm episodes found by other regional winter temperature reconstructions from the Himalayas and the Tibetan Plateau. Spatial correlation analysis with land surface temperatures revealed the spatial representativeness of our reconstruction for a larger geographical territory over the Himalayas and the Tibetan Plateau. Furthermore, winter temperature in the central Himalaya is teleconnected with the December-February India-Burma trough. The persistent increasing winter temperature in recent decades in the central Himalaya coincides with continental-scale warming. Alpine vegetation in humid regions of the Himalayas may benefit from winter warming via an earlier start and extension of the growing season, as long as moisture availability is sufficient.

1. Introduction

Plant growth and physiological processes in high-elevation mountain ecosystems are mainly constrained from periodically cold climate conditions (Alvarezuria and Körner, 2007; Körner et al., 2016; Maher et al., 2020). Low temperatures reduce radial growth and the carbon sink (direct growth limitation via slow cell-division rates) at high-elevation treeline, where the cold winters create chilling damage of fine roots and the cambial cells (Körner and Paulsen, 2004; Alvarezuria and Körner, 2007; Begum et al., 2013; Körner, 2012, 2015). Winter temperature strongly influences cambial activity and radial growth (Körner, 2012, 2015) and spring phenology events of woody plants in the alpine ecotones, such as bud break, leaf emergence and flowering (Fu et al., 2012; Ranjitkar et al., 2013; Basnett et al., 2019). Moreover, the variation in heat/chilling accumulation is the main driver of bloom timing (Guo et al., 2014). Changes in winter temperature conditions alter major ecological processes and fluxes, affecting water and carbon balance, advanced or retard phenology (Williams et al., 2015). However, detailed knowledge on high-elevation alpine vegetation response to winter conditions is still lacking (Kreyling, 2010; Dolezal et al., 2020). Information of annual-to-centennial variability of winter temperatures is relevant to evaluate long-term changes of ecosystem functioning and vegetation responses under global climate change.

High mountain ecosystems in the Himalayas are unique places to study climate variability and vegetation responses, since high-elevation Himalayan plant taxa of subalpine and alpine vegetation zones respond

* Corresponding author at: CAS Key Laboratory of Tropical Forest Ecology, Xishuangbanna Tropical Botanical Garden Chinese Academy of Sciences, Menglun, Mengla, Yunnan 666303, China.
E-mail address: fanzexin@xtbg.org.cn (Z.-X. Fan).

https://doi.org/10.1016/j.dendro.2020.125799
Received 26 April 2020; Received in revised form 30 November 2020; Accepted 16 December 2020
Available online 25 December 2020

more rapidly to changes in atmospheric temperatures and associated shifts in ecological processes (Liang et al., 2014; Panthi et al., 2017, 2020; Sigdel et al., 2018; Dolezal et al., 2020; Gaire et al., 2020a). The mountains of the Himalayas have been warming at an unprecedented rate of 0.5 °C per decade in past few decades (1951–2014, Sabin et al., 2020). This value is higher than in the surrounding lowlands (Mountain Research Initiative EDW Working Group, 2015), in the Arctic (0.112 °C/decade for 1998–2012, Huang et al., 2017), and of the mean global surface temperature trend (0.116 °C/decade for 2000–2014, Karl et al., 2015). Meanwhile, warming in Himalayas is more pronounced in the winter season as compared to other seasons (Sabin et al., 2020). Thus, better understanding on high-elevation vegetation responses to past climatic changes in the Himalayas can provide important insights to devise reliable projections of ongoing climate change, conservation planning of high-elevation ecosystems, and developing adaptation strategies. However, study of past climate variability and associated ecological processes in the Himalayas is challenging due to lack of long-spanned instrumental climate data, and thus needs to rely on proxy records such as tree-rings and shrub-rings.

Tree-rings and shrub-rings of high-elevation wood plant taxa serve as reliable high-resolution proxies across the world to record past climate changes on decadal-to-centennial scales. A substantial number of studies concerning climate variability and associated vegetation responses has been conducted in the Himalayan high mountains (Liang et al., 2014; Sigdel et al., 2018; Panthi et al., 2020). Dendrochronological approaches have been successfully applied for several conifer species (e.g., Cook et al., 2003; Sano et al., 2012; Panthi et al., 2017, 2020; Shah et al., 2019; Aryal et al., 2020; Gaire et al., 2020a, 2020b) and a few broad-leaved tree species (Liang et al., 2014, 2019; Tiwari et al., 2017; Sigdel et al., 2018). Meanwhile, dendrochronological studies using shrubs or dwarf-shrubs growth rings of both conifers and broad-leaved taxa at and above upper treelines are emerging across the world (Myers-Smith et al., 2011, 2015a, b). Globally, a substantial number of shrub-dendochronology based studies have been conducted in the alpine regions (e.g., Liang et al., 2015; Maher et al., 2020) including the Alps (Myers-Smith et al., 2011; Francon et al., 2020), and the Scandinavia (Bär et al., 2006, 2008), the Arctic (Rayback et al., 2012; Myers-Smith et al., 2015a; Opala-Owczarek et al., 2018), and the Tibetan Mountains (Liang and Eckstein, 2009; Li et al., 2013; Lu et al., 2015; Bi et al., 2017). Mostly, shrubs growth rings are relevant to study the alpine ecosystem response to global warming (Francon et al., 2020). Despite of the high biodiversity of the Himalayn region, extension of shrub-ring based dendroclimatology in the alpine ecosystem beyond the upper tree limit is still scarce (e.g., Liang et al., 2015; Huang et al., 2019; Wernicke et al., 2019; Pandey et al., 2020).

Several plant taxa distributed at the alpine treeline and above in the sub-nival vegetation zone (ca. 3900−4500 m a.s.l.) in the Himalayas provide unique opportunities to study vegetation response to climate shifts (Liang et al., 2015; Rayback et al., 2017; Pandey et al., 2020) and to reconstruct past climate variability. *Rhododendron* spp. are important shrub species distributed in the alpine and sub-nival vegetation zone of the Sino-Himalayan floristic region. Winter season temperature has been found to determine the vegetative and flowering phenology of *Rhododendron* spp., with strong positive relations via an earlier fulfillment of heat accumulation requirements (Ranjitkar et al., 2013; Basnett et al., 2019). Because of their longevity, *Rhododendron* spp. have high potential for reconstructing past climatic changes (Lu et al., 2015; Bi et al., 2017). The radial growth of high-elevation *Rhododendron* taxa is highly sensitive to annual and seasonal temperature changes under harsh environmental conditions at the upper alpine treeline and the sub-nival vegetation zone (Liang and Eckstein, 2009; Li et al., 2013). *Rhododendron campanulatum* is a dominant shrub species at upper treeline and above in alpine and sub-nival vegetation zone in the Himalayan region, yet the dendroclimatic potential of the species has not been explored.

The present study establishes a ring-width chronology of *R. campanulatum* for the first time from the central Himalaya. Our aims are: (a) to identify the climatic factors that limiting radial growth of *R. campanulatum* at the upper treeline, (b) to reconstruct the minimum winter temperature variability in the central Himalaya, (c) to investigate the teleconnections of minimum winter temperature change with large-scale climate drivers.

2. Materials and methods

2.1. Study area and climate

The study region is located at the alpine Krummholz treeline in the Mt. Gaurishankar massif of the Rolwaling Himal (Gaurishankar Conservation Area), central Himalaya, Nepal (Fig. 1). The study region is a high-elevation nature reserve and characterized by upper montane vegetation, which comprises evergreen coniferous cloud forests (*Abies spectabilis*, 3000−3900 m a.s.l.) and mixed broad-leaved montane forests (*Betula-Rhododendron*, 3600−3900 m a.s.l.), and dense shrubby thickets of *Rhododendron* spp. at and above alpine treeline (3900−4500 m a.s.l.) (Fig. S1, Miehe et al., 2015; Panthi, 2017).

The study region is dominated by the Indian summer monsoon climate, with warm and wet summers and cold winters (Böhner et al., 2015). About 75 % of the total annual precipitation falls during the summer monsoon season from June to September (Fig. 2a). The average annual maximum, mean, minimum temperatures, and total annual mean precipitation at Jiri station (27.63 °N, 86.23 °E, 2003 m a.s.l.) for the period 1975–2013 were 20.24 °C, 14.23 °C, 8.22 °C, and 2340 mm respectively (Fig. S2). Due to absence of instrumental records for our specific study area and the shortness of meteorological data of Jiri station located at the valley bottom ca. 40 km far from study site, we obtained monthly regional temperature and precipitation series from gridded data (27.5–28.5 °N/86−87 °E) at half-degree spatial resolution from the Climatic Research Unit (CRU, Harris et al., 2014). Mean maximum temperature in the warmest month (July) and minimum temperature in the coldest month (January) were 1.4 °C and -18.2 °C, respectively for regional CRU data (Fig. 2a), while that for Jiri station were 24.0 °C and -1.4 °C, respectively (Fig. S2). Regional CRU climate reveals that the study area is covered with snow from November to April (Fig. 2a). Mean annual temperature has increased significantly (0.184 °C/decade, period 1975–2013) at Jiri station, and at an even higher rate (0.285 °C/decade, period 1960–2013) for regional CRU data (Fig. 2b). No significant change has been observed for total annual precipitation at Jiri station during 1961–2013, and for regional CRU data during 1960–2013 (Fig. 2c).

2.2. Study species

Rhododendron campanulatum D. Don (Family *Ericaceae*) is an evergreen broad-leaved species and important component of the high-elevation Himalayan ecosystems at the upper treeline ecotone (Fang et al., 2005). The species flowers from April to May, and the fruit sets during July to September. The species is widely distributed in the Sino-Himalayan floristic region (Ward and Bamsbottom, 1927) mainly in the Himalayas (Kashmir-to-Bhutan) and South Tibet (Fig. 1; Fang et al., 2005). The species grows about 1.5–2.0 m tall at upper treeline and even shorter above treeline, while it grows as understory shrub up to 4.5 m tall below forestline in our study region. In our study region (Rolwaling valley) it forms a dense shrub thicket (single to multiple stems per trunk) at the Krummholz treeline on north facing open and steep moist mountain slopes as a pure-stand, while it associates with fir and birch at the forest-line (Schickhoff et al., 2014; Panthi, 2017). *R. campanulatum* prefers moist soil, and the aspects and slope with pronounced difference in moisture condition strongly affect its distribution. The species is frost-sensitive and adapted to extreme cold climate, and usually grows in well-drained sandy-to-loamy soil. The species is very important to form habitat for high-elevation flora and fauna and plays a crucial role to shelter several threatened endemic

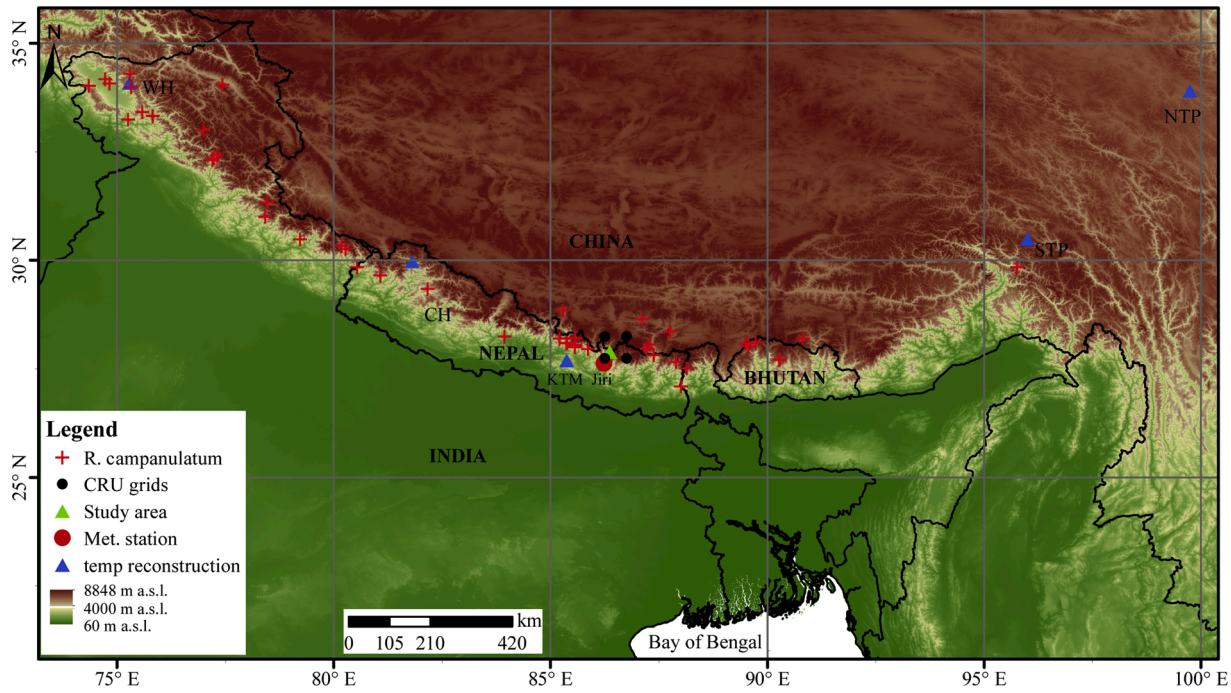

Fig. 1. Map of the study area showing topography, meteorological station (red circle), CRU grid points (black circles) and study area (green triangle) in the central Himalaya, Nepal. Blue triangles indicate five winter temperature reconstruction sites from the Himalayas (CH: Cook et al., 2003; Gaire et al., 2020b; WH: Shah et al., 2019) and the Tibetan Plateau (STP: Huang et al., 2019; NTP: Gou et al., 2007). Red crosses indicate locations of *Rhododendron campanulatum* within its natural distributional range, where herbarium specimens were collected (www.gbif.org).

species such as pheasants (Himalayan Moonal), Himalayan thar, Himalayan Jharal, Himalayan Goral, musk deer, etc.

2.3. Shrub ring data and chronology development

We collected increment cores of *Rhododendron campanulatum* at the upper Krummholz alpine treeline (3965 m) and above in the alpine meadow zone (4050 m) from Mt. Gaurishankar massif in the Rolwaling Himal section, Gaurishankar Conservation Area, East Nepal (Fig. 1). Due to the dense and uniform distribution of *R. campanulatum* across the mountain massif, we randomly established three 400 m^2 sized plots on steep slopes (40–45 degrees) at the upper alpine Krummholz treeline (3965−4050 m a.s.l.) (Fig. S1). We sampled all individuals of the study species occurring in these plots. We excluded talus slopes and other naturally disturbed sites (e.g., avalanche tracks and landslides) to avoid tree-ring width variations related to distortions by non-climatic signals. We collected two increment cores per stem (5.15-mm diameter) at about 0.5−0.7 m height above ground using an increment borer. The trunks of the species were leaning on a ground at the plots located in the upper treeline and forestline (Fig. S1). By sampling cores from upslope or lateral positions of the trunks, we avoided the possible impact of reaction wood related to compression on the descent position or tension on the upper side. Average stem diameter at sampling height was 13.5 cm, with a range from 9.0 cm to 24 cm (while diameter at breast height ranged between 8−23 cm). We followed standard procedures of dendrochronology for shrub-ring measurement and cross-dating (Stokes and Smiley, 1996). Prior to shrub-ring measurement, the wood surfaces of increment cores of *R. campanulatum* were polished to make ring boundaries clearly visible using sanding papers of successive grits i.e., from fine and up to ultra-fine (220–3000) grits. The species forms clear and distinct annual growth rings, with diffuse porous wood anatomical features i.e. vessels distributed uniformly over growth rings, and ring boundaries demarcated with a band of latewood fibers (Fig. S1d). Our sampling campaign was held in June 2014, and hence the complete annual growth rings are available up to 2013 for further analyses.

The annual growth rings of each increment core were measured with a resolution of 0.001 mm under the stereomicroscope (× 40 magnification) linked to a LINTAB digital positioning table (LINTAB™ 6, Rinntech, Germany). Each annual ring was cross-dated to the exact calendar year of their formation by visual growth pattern matching, and statistical tests: sign-test, *t*-test (t-value $\geq$ 3), cross-date index (CDI-value $\geq$ 20) and Gleichläufigkeit (glk-value $\geq$ 60) using the software package TSAP-Win (Stokes and Smiley, 1996; Rinn, 2003). Since Rhododendron forms irregular and asymmetric stems, cross-dating of discontinuous annual rings around the stem was challenging. Occurrence of extremely narrow-growth rings synchronized among the individuals; however, we did not find any false rings formation for the species. Prior to chronology development, we excluded series showing individual growth patterns related to competition and stand dynamics, and all series shorter than 55 years (mainly established after the year 1960) to avoid tree age/size related noise as well as to increase the climate signals in our chronology. In total, 53 cores from 31 individuals out of total 92 cores collected from 46 individual shrubs were used for further analyses (Table 1). We used the signal-free approach of age-dependent detrending (Melvin and Briffa, 2008) to standardize raw ring-width measurements to ring-width indices by using the program 'RCSSigfree' (http://www.ldeo.columbia.edu/tree–ring–laboratory/resources/software). We applied a data-adaptive power transformation to stabilize the age-related variance of raw measurement series and to minimize the potential influence of decreasing sample depths with time (Cook and Peters, 1997; Osborn et al., 1997). Each raw series was standardized by fitting an age-dependent 30-year spline detrending curve. After detrending, the index series were free of age-size related trends but still preserved low-to-medium frequency environmental signals (Melvin and Briffa, 2008). We developed the mean chronology by averaging each individually detrended series by calculating a bi-weight robust mean. We calculated basic statistical characteristics including mean sensitivity (MS), first-order autocorrelations (AC1), mean inter-series correlation (Rbar) and expressed population signal (EPS) to determine the chronology quality (Wigley et al., 1984; Briffa, 1995).

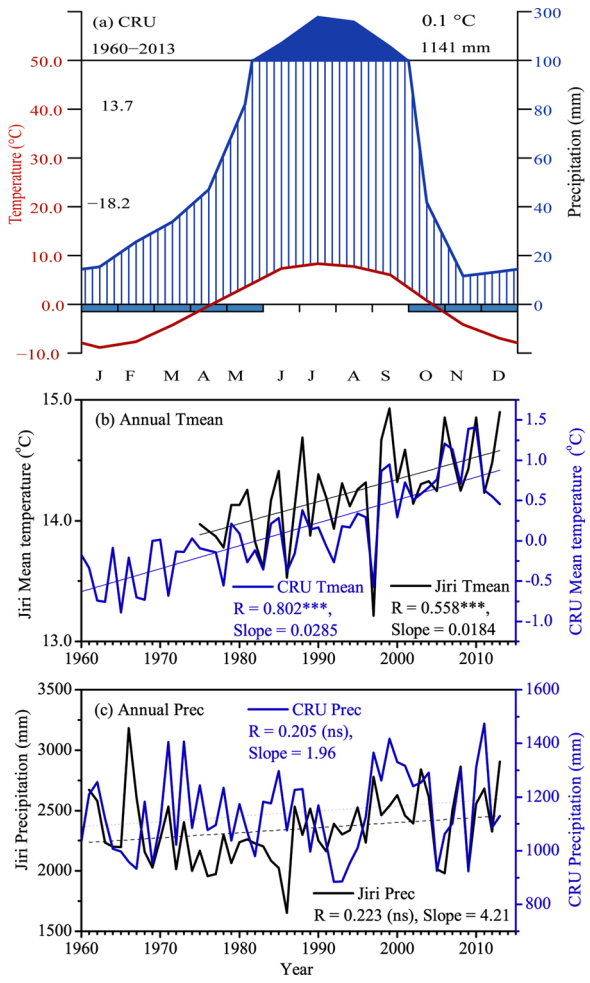

Fig. 2. Climate of the study area. (a) Walter and Lieth Regional CRU climograph showing monthly temperature (red line) and precipitation (blue line), (b) trends of mean annual temperature, and (c) trends of total annual precipitation. Climate trends twere analyzed for Jiri station (black line) and regional CRU data (blue line). The monthly mean maximum (13.7 °C, July, the warmest month) and minimum (-18.2 °C January, the coldest month) temperatures for regional CRU climate data was analyzed for the period 1960-2013. R, Pearson correlation coefficient over the time for series of station and CRU data; Slope, slope of trend line. Significance level: ***, $p < 0.001$; ns, not significant.

2.4. Climate data

We obtained the monthly temperature and precipitation data of Jiri station (the closest station to our study area) (Fig. 1) from the Department of Hydrology and Meteorology, Nepal. Besides, we obtained regional temperature and precipitation series from monthly gridded global CRU data (CRUTS4.04; 27.50–28.50 °N/86.00–87.00 °E; Harris et al., 2014; https://crudata.uea.ac.uk/cru/data/hrg) at half-degree spatial resolution. Meteorological records for CRU gridded temperature for the central Himalaya are available since 1960 (https://crudata.uea.ac.uk/cru/data/temperature/crutem4/station-data.htm), and hence we used gridded data for the period 1960–2013 for growth-climate relations and further analyses. Correlation statistics revealed significant positive correlations between mean annual temperature (r = 0.80***) and mean annual precipitation (r = 0.48**) of CRU gridded data and meteorological data of Jiri station for the period 1975–2013. As estimates of the regional moisture conditions, we used the Standardized Precipitation-Evapotranspiration Index (SPEI, Vicente-Serrano et al., 2010) extracted from CRU grids (CRUTS4.03, http://sac.csic.es/spei). We also obtained the CRU gridded Northern Hemisphere snow cover extent data at half-degree spatial resolution for the period 1967–2013 from NOAA National Centers for Environmental Information (https://data.nodc.noaa.gov/cgi-bin/iso?id=gov.noaa.ncdc:C00756). Furthermore, we derived the index of India-Burma trough (IBT) from positive vorticity at 700 hPa during December-February averaged over 15 °N–25 °N/80 °E–100 °E (Wang et al., 2011). IBT is the subtropical westerly trough (1E-05 S^{-1}) and mainly active with high frequencies during winter. IBT index measures the variations in wintertime climate anomalies over Himalaya, southeastern Tibetan Plateau, southern- and southeastern Asia. The IBT index was derived from National Centers for Environmental Prediction (NCEP) – National Center for Atmospheric Research (NCAR) reanalysis data at 2.5-degree spatial resolution (Kalnay et al., 1996; https://psl.noaa.gov/data/gridded/data.ncep.reanalysis.derived.html).

2.5. Statistical analyses

We computed bootstrapped correlation coefficients between standardized ring-width chronology of *R. campanulatum* and gridded CRU monthly climate data (temperatures, precipitation and SPEI) for a 15-month dendroclimatic window from previous August to October of the current year using the package 'bootRes' (Zang and Biondi, 2013) in R (R Core Team, 2020). Growth-climate relations with regional gridded climate data and station data were similar in direction, as well as those correlations were significant but the magnitude of correlation coefficients differed (data not shown). However, due to several missing values and shorter span of station climate data, we decided to use the gridded CRU data for further analyses. We also computed bootstrapped response function analysis between the standardized ring-width chronology and all climate parameters to overcome the influence of multicollinearity among monthly climate using the package 'bootRes'. Besides, we performed seasonal correlation analysis (SEASCORR, Meko et al., 2011) by aggregating monthly climate variables for 1, 3, 6 and 12 months. SEASCORR uses the partial correlations to compute the actual strength of the linear relationship of a primary variable after removing the effect of a secondary variable and vice-versa. We determined primary and secondary (temperature and precipitation) variables based on the outputs of bootstrapped correlations and response functions. Furthermore, the temporal stability of growth-climate relations was analyzed by computing correlations for 30-year moving windows for the period 1960–2013. The SEASCORR and moving correlation analysis were performed using the package 'treeclim' (Zang and Biondi, 2015) in R (R Core Team, 2020).

A linear regression model was developed as a transfer function (Fritts, 1976) between the ring-width chronology and seasonal climate (December-February minimum temperature) based on the calibration statistics obtained for the period 1960–2013. The calibration model was validated by several rigorous tests such as F-test, standard error (SE), and Durbin–Watson (DW) statistics for residual autocorrelation. The robustness of December-February minimum temperature reconstruction was verified using several rigorous statistics, e.g. sign-test (ST), product

Table 1
Site characteristics and chronology statistics of *Rhododendron campanulatum* in the Rolwaling Himal valley, central Himalaya. AGR, average growth rate; MSL, mean segment length; MS, mean sensitivity; AC1, first-order autocorrelation; Rbar, mean inter-series correlation; EPS, expressed population signal. AGR was calculated for raw series, while MS, AC1, Rbar, and EPS were calculated for standardized chronology after detrending.

Latitude (N)	Longitude (E)	Elevation (m a.s.l.)	Cores/Shrubs	Span	AGR (mm/yr)	MSL (yr)	MS	AC1	Rbar	EPS
27.89	86.37	3965−4050	53/31	1787–2013	0.618	125	0.282	0.547	0.3335	0.862

mean test (Pmt), reduction of error (RE), and root mean square error (RMSE) (Fritts, 1976; Michaelsen, 1987). Due to the relatively short span of the calibration period, we used the leave-one-out cross-validation approach (Michaelsen, 1987) for verification of reconstructed December-February minimum temperature. In this process, cross-validation is repeated iteratively, where one observation is removed in each step of calibration model. We investigated the spatial representative of our December-February minimum temperature reconstruction using spatial correlation analysis with global CRU gridded land temperature in field at half-degree spatial resolution. We performed spatial correlation analysis for the period 1960–2013 via KNMI Climate Explorer (Trouet and Oldenborgh, 2013; http://climexp.knmi.nl/) and mapped correlation coefficients at 95 % confidence interval.

3. Results

3.1. Chronology characteristics

Ring-width chronology of Himalayan shrub Rhododendron (*R. campanulatum*) spans the period 1787–2013, i.e. 227 years (Fig. 3) with a relatively low average radial growth rate (AGR =0.618 mm/year) (Table 1). Noticeable low growth periods were observed during 1800–1820, 1860–1880 s, 1910–1930 s and 1940s with extremely low growth during the 1870s. During 1890s-1970, growth fluctuated mostly below the mean, but after the 1960s growth trends increased continuously (Fig. 3). The values of mean sensitivity (MS = 0.282), and inter-series correlation (Rbar = 0.333) were moderate (Table 1). The high value of first-order autocorrelation (AC1 = 0.547) indicated impact of previous year's growth on current growth (Table 1). The expressed population signal (EPS) was 0.862 for the whole chronology period (1787–2013), while the running EPS surpassed the recommended threshold of 0.85 for the period 1845–2013 when a replication with 11 series or more was reached (Fig. 3).

3.2. Growth-climate relations

Bootstrapped correlation analysis indicated positive relationships between signal-free ring-width chronology and temperatures from previous November to current October (Fig. 4). Similarly, standardized ring-width chronology correlated positively with precipitation and SPEI (moisture availability) during May. The highest correlation was obtained with the December-February minimum (r = 0.781, $p < 0.001$) and mean (r = 0.751, $p < 0.001$) temperatures. Radial growth showed second highest positive relationships with August mean (r = 0.555, $p < 0.001$) and minimum (r = 0.525, $p < 0.001$) temperatures (Fig. 4). Bootstrapped response-function analyses revealed a very similar response pattern as the correlation analyses (in the same direction but with a lower magnitude), although response coefficients were significant only with temperatures of the months January and February, and May precipitation (Fig. S3). Results of partial correlation analyses computed with monthly and seasonal means of temperatures for the period 1960–2013 validated the strongest December-February minimum temperature sensitivity (Fig. 5), indicating that the winter minimum temperature strongly affects radial growth of *R. campanulatum* at the upper treeline in the central Himalaya. The moving correlation analysis further confirmed the consistency and temporal stability of the temperature sensitivity during the calibration period 1960–2013 (Fig. S4). Besides, radial growth showed significant negative relationships with regional snow cover extent (r = -0.651, $p < 0.001$) from previous year November to current April (Fig. S5).

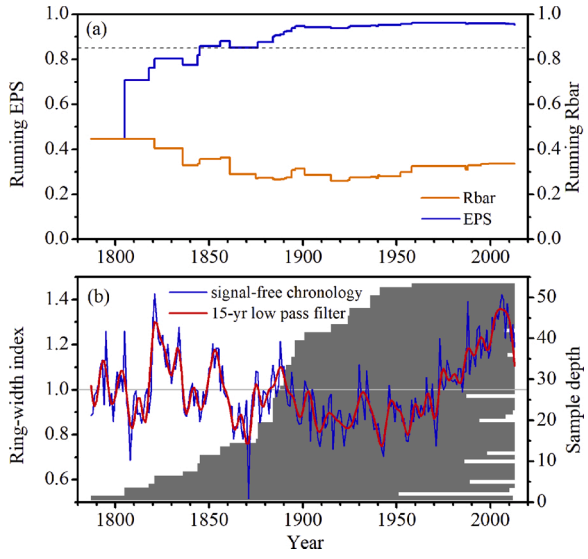

Fig. 3. Signal-free chronology of *Rhododendron campanulatum* from Rolwaling valley, central Himalaya, Nepal: (a) running Rbar and running EPS, and (b) shrub-ring chronology (blue line) with 15-year low pass filter (red line) and sample depth (grey shading).

3.3. Temperature reconstruction

The results of climate sensitivity and seasonal correlation (SEASCORR) analysis provided a basis to reconstruct winter (December-February) minimum temperature in central Himalaya from the *R. campanulatum* chronology. We developed a linear regression model ($Y_{Tmin} = 3.964 \times RWI - 21.512$, $p < 0.001$) with December-February minimum temperature (predictand) and the standardized chronology of Rhododendron as a predictor. The 'transfer function' model explained 61.0 % of the actual December-February minimum temperature variance during the calibration period 1960–2013 (Table 2, Fig. 6a), the high value of an F-test (81.23) confirmed the reliability of the calibration model. A negligible first-order positive autocorrelation (DW = 1.811, cf. 2.0) indicates normal distribution of regression residuals. The reconstruction dates back to 1845 and tracks well both high- and low-frequency variations of the actual minimum winter temperature (Fig. 6). Furthermore, the high positive value of RE (0.578), sign-test (+47/−7), and Pmt (4.015) of the verification tests signify the predictive skill, robustness and validity of our reconstruction. The RMSE value (0.532) was considerably smaller than the standard deviation of actual temperature (0.827) during the calibration period, indicating predictive skill of our model is not due to overfitting (Table 2). Further comparison of first-differences of actual and reconstructed temperatures revealed high-frequency consistencies (Fig. 6b), and significant verification statistics during 1961–2013 indicting the robustness of our reconstruction (Table 2).

The long-term mean of our reconstructed minimum winter temperature was –17.6 °C (Fig. 6c), indicating that the alpine treeline and the region beyond are under very cold stress during winter. Our reconstruction revealed several warm (mean + 1 standard deviation) and cold (mean - 1 standard deviation) periods of winter temperatures during the past 169 years (1845–2013). The reconstruction contained a total of 26 (15.38 %) extreme warm and 20 (11.83 %) extreme cold events (Fig. 6c, Table 3). Periods of warmer winters occurred during 1854−1855, 1993−1994, 1996−1998, and 2000−2013; while cold winters were found during 1908−1910, 1922−1923, 1941−1944, and 1955−1957. A very cold episode in our reconstruction occurred during 1860–1870 s (with 1871 as a coldest year), which is consistent with other reconstructions (Fig. 7b, e, f). After ca. 1960, the reconstruction revealed a continuous warming trend in the central Himalaya (Fig. 6c) that coincided with other regional temperature reconstructions (Fig. 7) and continental-scale warming.

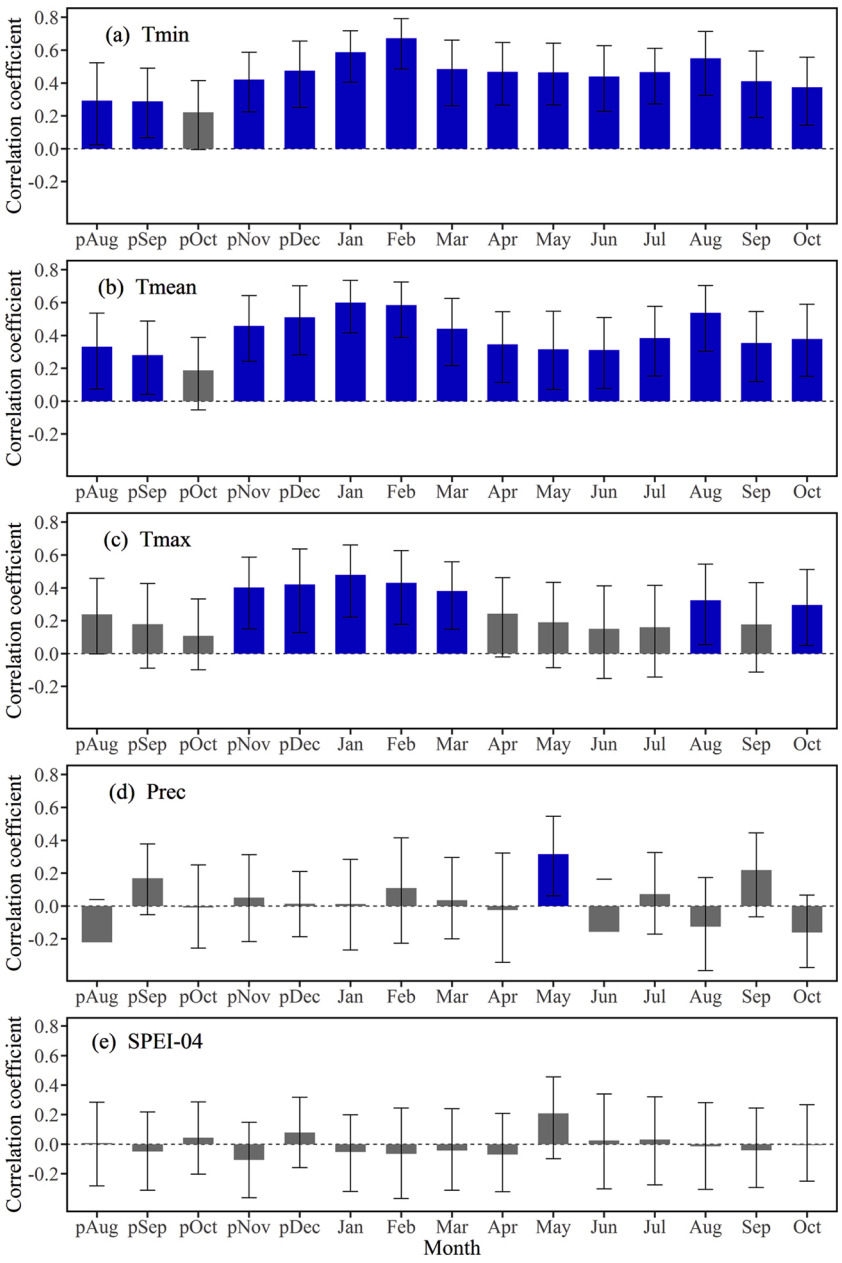

Fig. 4. Bootstrapped correlation analysis of standardized radial growth of *Rhododendron campanulatum* with regional CRU gridded monthly temperatures (Tmin, minimum; Tmean: mean; and Tmax, maximum), precipitation (Prec), and SPEI for the period 1960–2013. The vertical black lines in each bar represent upper and lower confidence intervals of correlation coefficients at the 95 % confidence level, while the blue and grey bars indicate statistically significant ($p < 0.05$) and non-significant ($p > 0.05$) correlation coefficients, respectively.

3.4. Spatial correlation and teleconnections

The spatial correlation analysis between the reconstructed December-February minimum temperature and CRU gridded minimum land temperature during December-February showed strong positive correlations across a large territory over the Himalaya including India, the Tibetan Plateau and vicinities (Fig. 8), and thus revealed possible influence of large-scale climate drivers on winter temperature variability in the Himalayan region. Further analysis of our reconstruction revealed a significant positive correlation ($r = 0.628$, $p < 0.001$) with the December-February IBT index (Fig. 9).

4. Discussion

Our study revealed that the radial growth of *R. campanulatum* is positively related to temperatures throughout the year, but strongly sensitive to winter (December-February) minimum temperature at the upper treeline in the central Himalaya (Figs. 4 and 5). The negative relations of radial growth with snow cover extent during November-May further supports the sensitivity of Rhododendron shrubs to winter temperature variations. The underlying reasons for this response include that the evergreen leaves and buds, and fine roots of Rhododendrons may suffer from frost damage under harsh frost conditions, which further alter the availability of stored carbohydrate for new tissues formation. In our study region, Panthi et al. (2020) observed that radial growth of *Abies spectabilis* at the upper treeline was sensitive to temperature variations during the winter months. Maher et al. (2020) revealed that winter damage primarily constrains plant growth at krummholz treeline, though growing season temperature helps to increase growth rate. Frost damage and snow cover extent also amplify chilling dormancy by altering the hormonal regulation to reactivate cambial activity (Begum et al., 2013), which ultimately reduces the plant's productivity after very cold winter conditions. Plant growth performance in mountain ecosystems depends on the conditions during winter (Kreyling, 2010), although low temperature limits carbon sink year-round (Alvarezuria and Körner, 2007). The plants in high-elevation

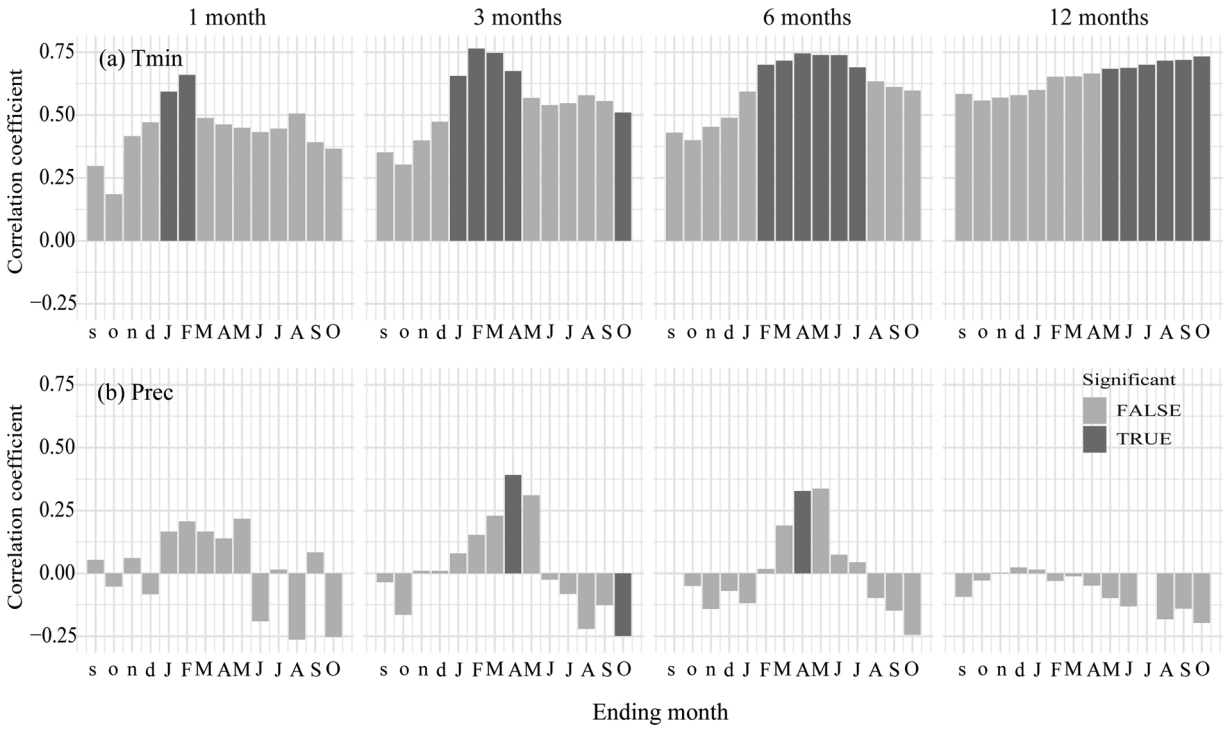

Fig. 5. Partial correlation analysis of standardized radial growth of *Rhododendron campanulatum* with time windows of monthly and seasonal means (1-, 3-, 6- and 12-months) computed for the common period 1960-2013: (a) minimum temperature (Tmin, upper panel) and (b) precipitation (Prec, lower panel). The letters on the x-axis represent months from previous September to current year October. The dark grey vertical bars represent the partial correlation coefficients derived from Monte-Carlo permutation at 95 % confidence level.

Table 2
Calibration and leave-one-out verification statistics of winter (December-February) minimum temperature reconstruction during the period 1960–2013. SE, standard error of estimates; DW, Durbin–Watson statistics; ST, sign test; Pmt, product-mean test; RE, reduction of error; RMSE, root-mean-square error.

Calibration model: $Y_{Tmin} = 3.964 \times RWI - 21.512$, $p < 0.001$						
Period	r	r^2	r^2_{adj}	F	SE	DW
1960–2013	0.781	0.6097	0.6022	81.231	0.521	1.811
Leave-one-out verification						
Period	r_{ver}	r^2_{ver}	ST	Pmt	RMSE	RE
1960–2013	0.761	0.579	+47/–7	4.015	0.532	0.578
First-difference verification						
Period	r_{ver}	r^2_{ver}	ST	Pmt	RMSE	RE
1961–2013	0.372	0.138	+32/-21	2.575	0.683	0.100

ecosystems have to cope with a very short growing season (Inouye and Wielgolaski, 2003; Körner, 2003). Climatic treelines are usually constrained by low temperature (Körner and Paulsen, 2004; Maher et al., 2020), and thus plant growth may benefit from an earlier start of cambial activity and extended growing season due to warming of minimum winter temperatures. Furthermore, winter warming affects spring phenology of alpine plants in high-elevation ecosystems via earlier snowmelt and soil thawing (Körner, 2003; Ranjitkar et al., 2013), and which ultimately supports soil moisture availability to start cambial activity.

Warmer winters foster an earlier fulfillment of requested heat accumulation sums for the start of cambial activity of alpine conifer tree species, like e.g. *Abies georgei* (Li et al., 2017), and the breaking of dormancy of temperate broad-leaved species (Guo et al., 2014). Besides, winter warming affects all other phenological processes, such as leaf/bud outbreak, flowering and fruiting of temperate and alpine plants including conifers, broad-leaved shrubs and trees (Fu et al., 2012; Ranjitkar et al., 2013; Hollesen et al., 2015; Williams et al., 2015), and plant growth dynamics in Himalayan alpine forbs (Dolezal et al., 2020). A positive radial growth response of high-elevation Himalayan taxa to winter temperatures is supported by several studies conducted at upper alpine forestline or treeline, as well as in the temperate elevation belt in the Himalayas (Shah et al., 2019; Gaire et al., 2020a, b; Panthi et al., 2020), on the Tibetan Plateau, and in the Hengduan Mountains (Bräuning, 2006; Fan et al., 2009; Panthi et al., 2018; Huang et al., 2019). Dolezal et al. (2020) observed that warm (snowy) winters support (reduce) plant growth and recruitment dynamics of an alpine forb *Potentilla pamirica* at the upper alpine treeline and in the sub-nival zone in the western Himalayas.

The explained variance of our December-February minimum temperature reconstruction (61 % of actual temperature) is comparable to, or even higher than previous climate reconstructions from the Himalayas and nearby regions (Cook et al., 2003; Panthi et al., 2017; Shah et al., 2019; Gaire et al., 2020b; Zaw et al., 2020). Our reconstruction reveals extreme cold periods during the past 169 years in the central Himalaya (Fig. 6c). The reconstructed December-February minimum temperature reveals inter-annual to decadal variations in temperature during past 169 years (1845–2013). Periods of high and low minimum temperatures in the central Himalaya are consistent with warm-cool episodes in other regional tree-ring derived temperature reconstructions (mainly at decadal scale) from the Himalayas (Cook et al., 2003; Shah et al., 2019; Gaire et al., 2020b), the Tibetan Plateau and vicinities in the Northern Hemisphere (Bräuning, 2006; Gou et al., 2007; Zhang et al., 2015; Bi et al., 2017; Huang et al., 2019). Very cold winters during 1860 s–1880 s (extremely low temperature in 1870s) was prominent in Northern hemisphere (Bräuning, 2006; Gou et al., 2007; Duan et al., 2012; Gaire et al., 2020b). Panthi et al. (2020) also observed reduced tree-growth of *Abies spectabilis* during 1860 s–1880 s at the upper alpine treeline in our study region. The extreme low temperature during the 1870s (the lowest in 1871) across a wider region (in Himalaya and Tibetan Plateau) is probably related to cooling effects of large

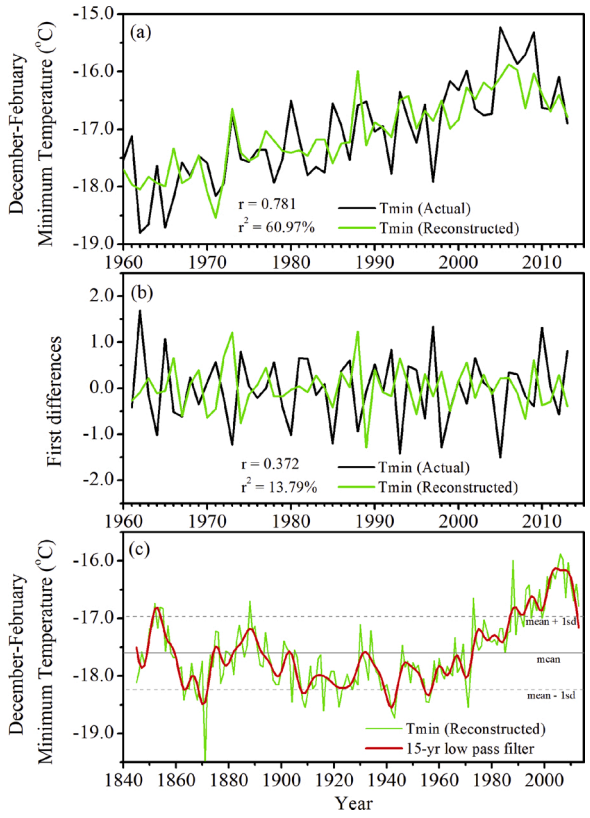

Fig. 6. December-February minimum temperature reconstruction for the central Himalaya, Nepal. (a) Comparison between actual and reconstructed December-February minimum temperature during the calibration period 1960–2013, (b) comparison between the first-differenced data of actual and reconstructed December–February minimum temperature, and (c) reconstructed December-February minimum temperature series (green line) and 15-yr low-pass filter (thick red line) during 1845–2013. The horizontal grey line represents the long-term mean of the reconstructed series; and the dashed grey lines represent ± 1 standard deviations.

Table 3
Extreme warm and cool events in the central Himalaya exceeding ± 1 standard deviation from the mean of the December-February minimum temperature reconstruction.

Extreme warm		Extreme cold	
Years	1852, 1854, 1855, 1888, 1973, 1988, 1990, 1993, 1994, 1996, 1997, 1998, 2000, 2001, 2002, 2003, 2004, 2005, 2006, 2007, 2008, 2009, 2010, 2011, 2012, 2013 (Total 26 years)	Years	1863, 1868, 1871, 1904, 1908, 1909, 1910, 1916, 1922, 1923, 1927, 1938, 1941, 1942, 1943, 1944, 1955, 1956, 1957, 1971 (Total 20 years)
Periods	1854–1855, 1993–1994, 1996–1998, 2000–2013	Periods	1908–1910, 1922–1923, 1941–1944, 1955–1957

volcanic eruptions (e.g. Iceland eruption) (Gaire et al., 2020b). Meanwhile, the slight variation in magnitude and duration of warm-cool episodes among compared reconstructions is probably related to a reconstruction window of different months for mean and minimum temperatures.

The warming trend in minimum winter temperature in the central Himalaya is persistent in recent decades, and the phenomenon coincides with other regional climate reconstructions from nearby regions (Gou et al., 2007; Bi et al., 2017; Huang et al., 2019; Shah et al., 2019; Gaire et al., 2020b) and continental-scale warming. Furthermore, the minimum winter temperature changes in the central Himalaya reveal strong

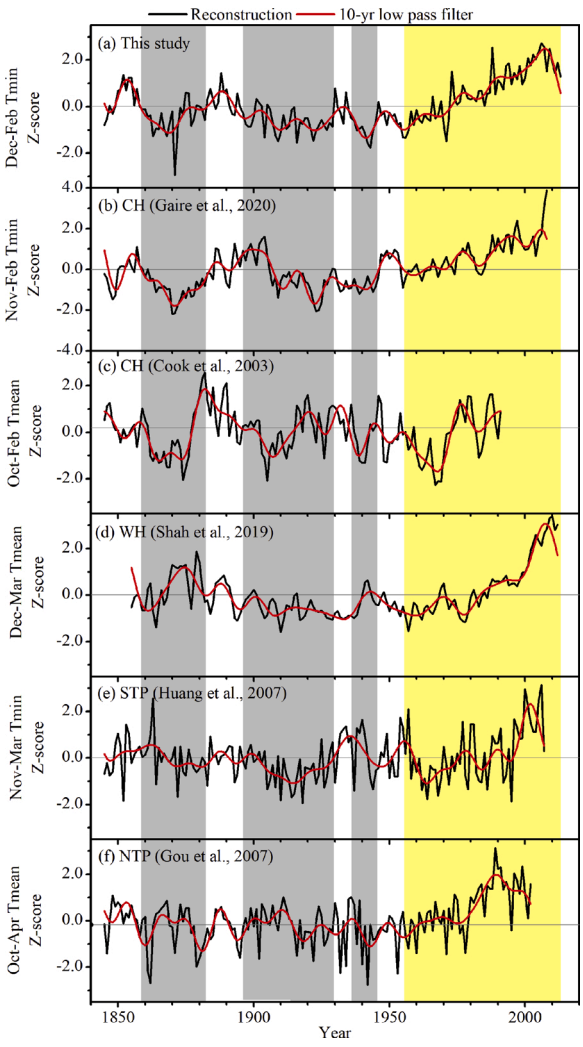

Fig. 7. Comparison of winter temperature reconstructions from the Himalayas and the Tibetan Plateau: (a) December–February minimum temperature in the central Himalaya (this study), (b) November-February minimum temperature (CH; Gaire et al., 2020b), (c) October-February mean temperature (CH; Cook et al., 2003), (d) December-March mean temperature (WH; Shah et al., 2019), (e) November-March minimum temperature (STP; Huang et al., 2019), and (f) October-April minimum temperature (NTP, Gou et al., 2007). CH, central Himalaya; WH, western Himalaya; STP, southeastern Tibetan Plateau; NTP, northeastern Tibetan Plateau. We used standardized values (Z-score) of each reconstruction for easier comparison. The vertical grey shadings denote cool episodes and the yellow shading indicates the recent persistent winter warming.

coherent associations with the India-Burma trough (Fig. 9). The consistency between our reconstruction and IBT index indicates a coherent teleconnection of minimum winter temperature variability with the India-Burma Trough. Zhang et al. (2015) has also observed strong positive association between IBT and minimum autumn-winter temperature in the eastern Tibetan Plateau. Stronger IBT due to positive vorticity leads the expansion of the warm tropical flow from south-to-north as well as the retraction of the cold high-latitude flow via stronger anticyclonic pattern (Wang et al., 2011; Zhang et al., 2015). The IBT during winter (December-February) affects the climate over larger geographical region including Himalaya, southeastern Tibetan Plateau, and southern- and southeastern Asia. Recent winter warming in the central Himalaya is thus related to short troughs carrying warm air flow with stronger anticyclonic pattern with increasing positive vorticity over India-Burma region.

This study reveals the high potential of Rhododendron shrubs

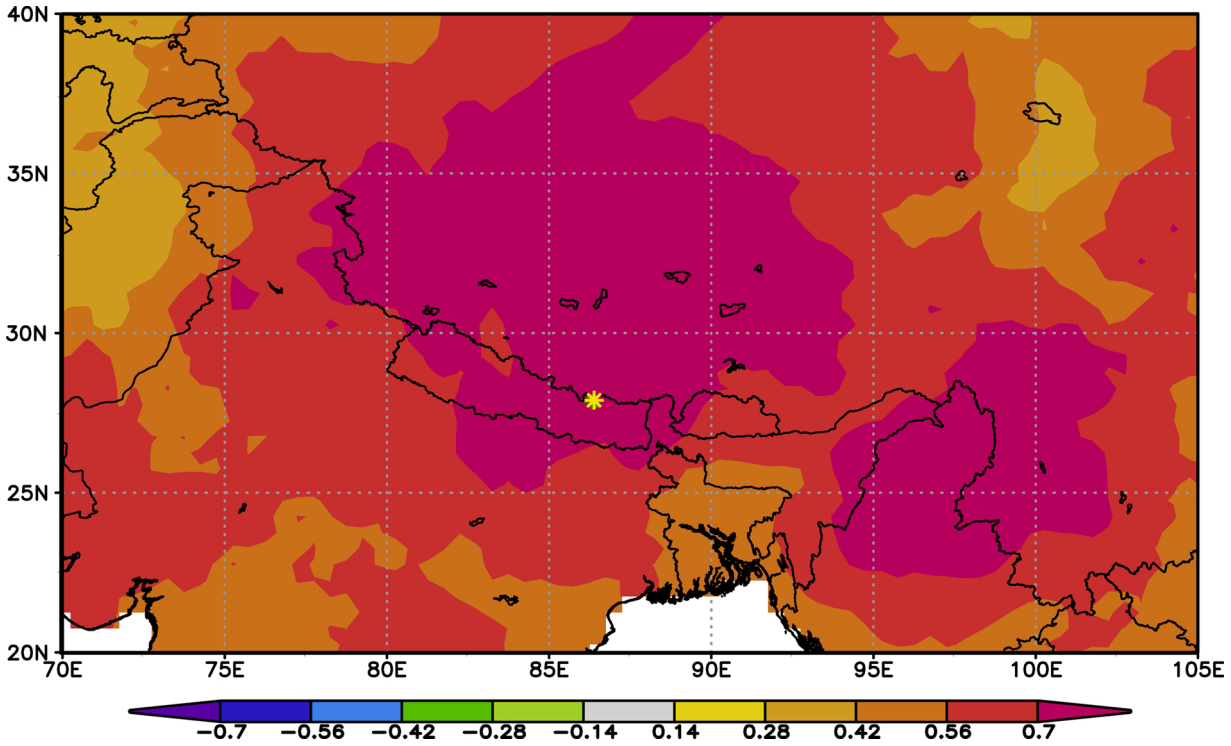

Fig. 8. Spatial correlation analysis of reconstructed December-February minimum temperature with CRU land minimum temperature at half-degree spatial resolution. Pearson correlation coefficients were computed with December-February temperatures for the period 1960–2013 via KNMI climate explorer (https://climexp.knmi.nl). Horizontal color bar represents the scale of correlation coefficients. Only statistically significant values ($p \leq 0.05$) were mapped. Asterisk (*) represents our study region.

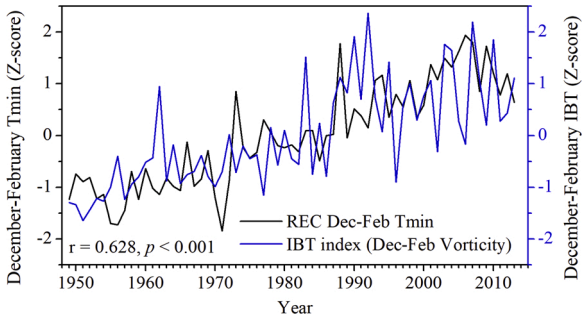

Fig. 9. Comparison of reconstructed December-February minimum temperature with December–February India-Burma Trough index. We used standardized values (Z-score) of both series for easier comparison.

growth-rings to reconstruct past winter temperature changes in the Himalayan region based on the dendroclimatic verification. The Himalayan region is still lacking the long-spanned instrumental climate data and empirical data on alpine vegetation response to climatic changes, where several taxa are sensitive to seasonal (mainly winter) temperature change for their radial growth and spring phenology. Constant warming of winter temperature may alter the radial growth and may lead to a seasonal shift in spring phenology of the upper montane vegetation in the Himalaya. Climate projection analyses under different Representative Concentration Pathway (RCP) scenarios revealed significant decrease in winter snow cover and increase in wintertime temperatures (3.5 ± 1.4 °C to 5.1 ± 1.8 °C) in the 21st century over the Himalayas (Sabin et al., 2020). Enhanced Rhododendron shrubs growth under warming may facilitate upward shifts of alpine vegetation via modification of micro-environmental conditions (Chen et al., 2020; Francon et al., 2020). However, if climate warming continues at the same rate and warming-induced moisture-stress is coupled with increasing year-to-year variability of moisture conditions, growth and productivity of high-elevation Himalayan plants could become increasingly vulnerable at their lower distributional range and in drier regions (Dolezal et al., 2020; Panthi et al., 2020).

5. Conclusions

This study demonstrated the high dendroclimatic potential of *R. campanulatum* beyond upper tree limit from the central Himalaya. A 227-year long ring-width chronology of *R. campanulatum* documents the high longevity of this species. Growth-climate relations revealed that radial growth of *R. campanulatum* in alpine vegetation beyond upper treeline is strongly sensitive to low winter temperature. A robust reconstruction on minimum winter temperature was established for the past 169 years in the central Himalayan region. The coherent association of minimum winter temperature variability with IBT index provides an evidence on possible influence of the stronger India-Burma trough on winter climate of the Himalaya. Our results imply that growth of *R. campanulatum* may benefit from future winter warming, and thus potential upslope expansion of alpine vegetation under sufficient soil moisture conditions. Our results demonstrated that Rhododendron shrub-ring chronology can be used as a high-resolution proxy for studying long-term environmental changes in the Himalayan alpine vegetation

Declaration of Competing Interest

We declare no competing financial and any other potential conflict of interests.

Acknowledgements

This work was funded by the National Natural Science Foundation of China (NSFC, 31861133007, 31770533), National Key Research

Development Program of China (2016YFC0502105) and the CAS 135 program (2017XTBG-T01). SP was supported by 'The CAS President's International Fellowship Initiative' (PIFI) postdoctoral fellowship (2019PC0104). We acknowledge Gaurishankar Conservation Area for providing permission for field sampling. We thank Prof. Edward Cook, Prof. Xiao-hua Gou, Dr. Santosh Shah, Dr. Ru Huang and Dr. Narayan Gaire for sharing their tree-ring reconstructions. We acknowledge Prof. Udo Schickhoff for providing permission to reproduce picture of Krummholz treeline (Fig. S1b). Dr. Janardan Mainali, and Mr. Rajesh Tamang are thankful for their help during the field work. Meteorological data of Jiri station was obtained from Department of Hydrology and Meteorology, Nepal.

Appendix A. Supplementary data

Supplementary material related to this article can be found, in the online version, at doi:https://doi.org/10.1016/j.dendro.2020.125799.

References

Alvarezuria, P., Körner, C., 2007. Low temperature limits of root growth in deciduous and evergreen temperate tree species. Funct. Ecol. 21 (2), 211–218. https://doi.org/10.1111/j.1365-2435.2007.01231.x.

Aryal, S., Gaire, N.P., Pokhrel, N.R., Rana, P., Sharma, B., Kharal, D.K., et al., 2020. Spring season in Western Nepal Himalaya is not yet warming: a 400-year temperature reconstruction based on tree-ring widths of Himalayan Hemlock (*Tsuga dumosa*). Atmosphere 11 (2), 132. https://doi.org/10.3390/atmos11020132.

Bär, A., Bräuning, A., Löffler, J., 2006. Dendroecology of dwarf shrubs in the high mountains of Norway – a methodological approach. Dendrochronologia 24, 17–27. https://doi.org/10.1016/j.dendro.2006.05.001.

Bär, A., Pape, R., Bräuning, A., Löffler, J., 2008. Growth-ring variations of dwarf shrubs reflect regional climate signals in alpine environments rather than topoclimatic differences. J. Biogeogr. 35, 625–636. https://doi.org/10.1111/j.1365-2699.2007.01804.x.

Basnett, S., Nagaraju, S.K., Ravikanth, G., Devy, S.M., 2019. Influence of phylogeny and abiotic factors varies across early and late reproductive phenology of Himalayan Rhododendrons. Ecosphere 10 (1), e02581. https://doi.org/10.1002/ecs2.2581.

Begum, S., Nakaba, S., Yamagishi, Y., Oribe, Y., Funada, R., 2013. Regulation of cambial activity in relation to environmental conditions: understanding the role of temperature in wood formation of trees. Physiol. Plant. 147 (1), 46–54. https://doi.org/10.1111/j.1399-3054.2012.01663.x.

Bi, Y., Xu, J., Yang, J., Li, Z., Gebrekirstos, A., Liang, E., Yang, X., 2017. Ring-widths of the above tree-line shrub Rhododendron reveal the change of minimum winter temperature over the past 211 years in Southwestern China. Clim. Dyn. 48 (1), 3919–3933. https://doi.org/10.1007/s00382-016-3311-4.

Böhner, J., Miehe, G., Miehe, S., Nagy, L., 2015. Climate and weather. In: Miehe, G., Pendry, C.A., Chaudhary, R.P. (Eds.), Nepal: An Introduction to the Natural History, Ecology and Human Environment of the Himalayas. Royal Botanic Garden, Edinburgh, UK, pp. 385–472.

Bräuning, A., 2006. Tree-ring evidence of "Little Ice Age" glacier advances in southern Tibet. Holocene 16 (3), 369–380. https://doi.org/10.1191/0959683606hl922rp.

Briffa, K.R., 1995. Interpreting high-resolution proxy climate data, the example of dendroclimatology. In: von Storch, H., Navarra, A. (Eds.), Analysis of Climate Data Variability, Applications of Statistical Techniques. Springer, New York, pp. 77–94.

Chen, J., Yang, Y., Wang, S., Sun, H., Schob, C., 2020. Shrub facilitation promotes selective tree establishment beyond the climatic treeline. Sci. Total Environ. 708, 134618 https://doi.org/10.1016/j.scitotenv.2019.134618.

Cook, E.R., Peters, K., 1997. Calculating unbiased tree-ring indices for the study of climatic and environmental change. Holocene 7 (3), 361–370. https://doi.org/10.1177/095968369700700314.

Cook, E.R., Krusic, P.J., Jones, P.D., 2003. Dendroclimatic signals in long tree-ring chronologies from the Himalayas of Nepal. Int. J. Climatol. 23, 707–732. https://doi.org/10.1002/joc.911.

Dolezal, J., Jandova, V., Macek, M., Mudrak, O., Altman, J., Schweingruber, F.H., Liancourt, P., 2020. Climate warming drives Himalayan alpine plant growth and recruitment dynamics. J. Ecol. https://doi.org/10.1111/1365-2745.13459.

Duan, J., Zhang, Q.B., Lv, L., Zhang, C., 2012. Regional-scale winter-spring temperature variability and chilling damage dynamics over the past two centuries in southeastern China. Clim. Dyn. 39 (3), 919–928. https://doi.org/10.1007/s00382-011-1232-9.

Fan, Z.-X., Bräuning, A., Cao, K.-F., Zhu, S.-D., 2009. Growth-climate responses of high-elevation conifers in the central Hengduan Mountains region, southwestern China. For. Ecol. Manage. 258, 306–313. https://doi.org/10.1016/j.foreco.2009.04.017.

Fang, M., Fang, R., He, M., Hu, L., Yang, H., Chamberlain, D.F., 2005. Rhododendron. In: Wu, Z.-Y., Raven, P.H., Deyuan, H. (Eds.), Flora of China Volume 14: Apaiaceae Through Ericaceae. Science Press Beijing and Missouri Botanical Garden Press, St. Louis, pp. 260–455.

Francon, L., Corona, C., Till-Bottraud, I., Choler, P., Carlson, B.Z., Charrier, G., Améglio, T., Morin, S., Eckert, N., Roussel, E., Lopez-Saez, J., Stoffel, M., 2020. Assessing the effects of earlier snow melt-out on alpine shrub growth: the sooner the better? Ecol. Indic. 115, 106455 https://doi.org/10.1016/j.ecolind.2020.106455.

Fritts, H.C., 1976. Tree Rings and Climate. Cambridge University Press, Cambridge.

Fu, Y.H., Campioli, M., Deckmyn, G., Janssens, I.A., 2012. The impact of winter and spring temperatures on temperate tree budburst dates: results from an experimental climate manipulation. PLoS One 7 (10), e47324. https://doi.org/10.1371/journal.pone.0047324.

Gaire, N.P., Fan, Z.-X., Bräuning, A., Panthi, S., Rana, P., Shrestha, A., Bhuju, D.R., 2020a. *Abies spectabilis* shows stable growth relations to temperature, but changing response to moisture conditions along an elevation gradient in the central Himalaya. Dendrochronologia 60, 125675. https://doi.org/10.1016/j.dendro.2020.125675.

Gaire, N.P., Fan, Z.-X., Shah, S.K., Thapa, U.K., Rokaya, M.B., 2020b. Tree-ring record of winter temperature from Humla, Karnali, in central Himalaya: a 229 years-long perspective for recent warming trend. Geogr. Ann. Ser. A Phys. Geogr. https://doi.org/10.1080/04353676.2020.1751446.

Gou, X.H., Chen, F.H., Jacoby, G.D., Cook, E., Yang, M.X., Peng, H.F., Zhang, Y., 2007. Rapid tree growth with respect to the last 400 years in response to climate warming, northeastern Tibetan Plateau. Int. J. Climatol. 27 (11), 1497–1503. https://doi.org/10.1002/joc.1480.

Guo, L., Dai, J., Ranjitkar, S., Yu, H., Xu, J., Luedeling, E., 2014. Chilling and heat requirements for flowering in temperate fruit trees. Int. J. Biometeorol. 58 (6), 1195–1206. https://doi.org/10.1007/s00484-013-0714-3.

Harris, I., Jones, P.D., Osborn, T.J., Lister, D.H., 2014. Updated high-resolution grids of monthly climatic observations – the CRU TS3.10 dataset. Int. J. Climatol. 34, 623–664. https://doi.org/10.1002/joc.3711.

Hollesen, J., Buchwal, A., Rachlewicz, G., Hansen, B.U., Hansen, M.O., Stecher, O., Elberling, B., 2015. Winter warming as an important co-driver for Betula nana growth in western Greenland during the past century. Glob. Chang. Biol. 21 (6), 2410–2423. https://doi.org/10.1111/gcb.12913.

Huang, J., Zhang, X., Zhang, Q., Lin, Y., Hao, M., Luo, Y., Zhao, Z., Yao, Y., Chen, X., Wang, L., Nie, S., Yin, Y., Xu, Y., Zhang, J., 2017. Recently amplified arctic warming has contributed to a continual global warming trend. Nat. Clim. Chang. 7 (12), 875–879. https://doi.org/10.1038/s41558-017-0009-5.

Huang, R., Zhu, H., Liang, E., Liu, B., Shi, J., Zhang, R., Griesinger, J., 2019. A tree ring-based winter temperature reconstruction for the southeastern Tibetan Plateau since 1340 CE. Clim. Dyn. 53, 3221–3233. https://doi.org/10.1007/s00382-019-04695-3.

Inouye, D.W., Wielgolaski, F.E., 2003. High altitude climates. In: M. D, Schwartz (Ed.), Phenology: An Integrative Environmental Science. Kluwer Academic Publishers, pp. 195–214.

Kalnay, E., Kanamitsu, M., Kistler, R., Collins, W.D., Deaven, D.G., Gandin, L.S., Joseph, D., 1996. The NCEP/NCAR 40-year reanalysis project. Bull. Am. Meteorol. Soc. 77 (3), 437–471. https://doi.org/10.1175/1520-0477(1996)077<0437:TNYRP>2.0.CO;2.

Karl, T.R., Arguez, A., Huang, B., Lawrimore, J.H., Mcmahon, J., Menne, M.J., Zhang, H., 2015. Possible artifacts of data biases in the recent global surface warming hiatus. Science 348 (6242), 1469–1472. https://doi.org/10.1126/science.aaa5632.

Körner, C., 2003. Alpine Plant Life: Functional Plant Ecology of High Mountain Ecosystem, 2nd ed. Springer, New York. p 344.

Körner, C., 2012. Alpine Treelines: Functional Ecology of the Global High Elevation Tree Limits. Springer, Basel, Switzerland.

Körner, C., 2015. Paradigm shift in plant growth control. Curr. Opin. Plant Biol. 25, 107–114. https://doi.org/10.1016/j.pbi.2015.05.003.

Körner, C., Paulsen, J., 2004. A world-wide study of high altitude treeline temperatures. J. Biogeogr. 31 (5), 713–732. https://doi.org/10.1111/j.1365-2699.2003.01043.x.

Körner, C., Basler, D., Hoch, G., Kollas, C., Lenz, A., Randin, C.F., Zimmermann, N.E., 2016. Where, why and how? Explaining the low temperature range limits of temperate tree species. J. Ecol. 104 (4), 1076–1088. https://doi.org/10.1111/1365-2745.12574.

Kreyling, J., 2010. Winter climate change: a critical factor for temperate vegetation performance. Ecology 91, 1939–1948. https://doi.org/10.1890/09-1160.1.

Li, Z., Liu, G., Fu, B., Zhang, Q., Ma, K., Pederson, N., 2013. The growth-ring variations of alpine shrub *Rhododendron przewalskii* reflect regional climate signals in the alpine environment of Miyaluo Town in Western Sichuan Province, China. Acta Ecol. Sin. 33 (1), 23–31. https://doi.org/10.1016/j.chnaes.2012.12.004.

Li, X., Liang, E., Gricar, J., Rossi, S., Cufar, K., Ellison, A.M., 2017. Critical minimum temperature limits xylogenesis and maintains treelines on the southeastern Tibetan Plateau. Chin. Sci. Bull. 62 (11), 804–812. https://doi.org/10.1016/j.scib.2017.04.025.

Liang, E., Eckstein, D., 2009. Dendrochronological potential of the alpine shrub Rhododendron nivale on the south-eastern Tibetan Plateau. Ann. Bot. 104 (4), 665–670. https://doi.org/10.1093/aob/mcp158.

Liang, E., Dawadi, B., Pederson, N., Eckstein, D., 2014. Is the growth of birch at the upper timberline in the Himalayas limited by moisture or by temperature? Ecology 95 (9), 2453–2465. https://doi.org/10.1890/13-1904.1.

Liang, E., Liu, W., Ren, P., Dawadi, B., Eckstein, D., 2015. The alpine dwarf shrub *Cassiope fastigiata* in the Himalayas: does it reflect site-specific climatic signals in its annual growth rings? Trees-Struct. Funct. 29 (1), 79–86. https://doi.org/10.1007/s00468-014-1128-5.

Liang, E., Dawadi, B., Pederson, N., Piao, S., Zhu, H., Sigdel, S.R., Chen, D., 2019. Strong link between large tropical volcanic eruptions and severe droughts prior to monsoon in the central Himalayas revealed by tree-ring records. Chin. Sci. Bull. 64 (14), 1018–1023. https://doi.org/10.1016/j.scib.2019.05.002.

Lu, X., Camarero, J.J., Wang, Y., Liang, E., Eckstein, D., 2015. Up to 400-year-old Rhododendron shrubs on the southeastern Tibetan Plateau: prospects for shrub-based dendrochronology. Boreas 44 (4), 760–768. https://doi.org/10.1111/bor.12122.

Maher, C.T., Nelson, C.R., Larson, A.J., 2020. Winter damage is more important than summer temperature for maintaining the krummholz growth form above alpine treeline. J. Ecol. 108 (3), 1074–1087. https://doi.org/10.1111/1365-2745.13315.
Meko, D.M., Touchan, R., Anchukaitis, K.J., 2011. SEASCORR: a MATLAB program for identifying the seasonal climate signal in an annual tree-ring time series. Comput. Geosci. 37, 1234–1241. https://doi.org/10.1016/j.cageo.2011.01.013.
Melvin, T.M., Briffa, K.R., 2008. A signal–free approach to dendroclimatic standardization. Dendrochronologia 26 (2), 71–86. https://doi.org/10.1016/j.dendro.2007.12.001.
Michaelsen, J., 1987. Cross-validation in statistical climate forecast models. J. Clim. Appl. Meteorol. 26 (11), 1589–1600. https://doi.org/10.1175/1520-0450(1987)026<1589:Cviscf>2.0.Co;2.
Miehe, S., Bäumler, R., Ghimire, S.K., Bhatrarai, K.R., Chaudhary, R.P., Subedi, M., Pendry, C., 2015. Vegetation ecology. In: Miehe, S., Pendry, C.A. (Eds.), Nepal: An Introduction to the Natural History, Ecology and Human Environment in the Himalayas, 1st ed. Royal Botanical Garden Edinburgh, Edinburgh, UK, pp. 385–472.
Myers-Smith, I.H., Forbes, B.C., Wilmking, M., Hallinger, M., Lantz, T.C., Blok, D., Hik, D. S., 2011. Shrub expansion in tundra ecosystems: dynamics, impacts and research priorities. Environ. Res. Lett. 6 (4), 045509. https://doi.org/10.1088/1748-9326/6/4/045509.
Myers-Smith, I.H., Elmendorf, S.C., Beck, P.S., Wilmking, M., Hallinger, M., Blok, D., Vellend, M., 2015a. Climate sensitivity of shrub growth across the tundra biome. Nat. Clim. Chang. 5 (9), 887–891. https://doi.org/10.1038/nclimate2697.
Myers-Smith, I.H., Hallinger, M., Blok, D., Sassklaassen, U., Rayback, S.A., Weijers, S., Wilmking, M., 2015b. Methods for measuring arctic and alpine shrub growth: a review. Earth. Rev. 140, 1–13. https://doi.org/10.1016/j.earscirev.2014.10.004.
Opala-Owczarek, M., Piroznikow, E., Owczarek, P., Szymanski, W., Luks, B., Kepski, D., Migala, K., 2018. The influence of abiotic factors on the growth of two vascular plant species (*Saxifraga oppositifolia* and *Salix polaris*) in the High Arctic. Catena 163, 219–232. https://doi.org/10.1016/j.catena.2017.12.018.
Osborn, T.J., Biffa, K., Jones, P., 1997. Adjusting variance for sample-size in tree-ring chronologies and other regional-mean timeseries. Dendrochronologia 15, 89–99.
Pandey, J., Sigdel, S.R., Lu, X., Salerno, F., Dawadi, B., Liang, E., Camarero, J.J., 2020. Early growing-season precipitation drives radial growth of alpine juniper shrubs in the central Himalayas. Geografiska Annaler: Ser. A, Phys. Geogr. https://doi.org/10.1080/04353676.2020.1761097.
Panthi, S., 2017. Long-term Tree Growths and Their Responses to Global Changes along Elevation Gradients in the Central Himalaya and Hengduan Mountains. PhD dissertation. Xishuangbanna Tropical Botanical Garden, Chinese Academy of Sciences, Xishuangbanna, China.
Panthi, S., Bräuning, A., Zhou, Z., Fan, Z.-X., 2017. Tree rings reveal recent intensified spring drought in the central Himalaya, Nepal. Glob. Planet. Change 157, 26–34. https://doi.org/10.1016/j.gloplacha.2017.08.012.
Panthi, S., Bräuning, A., Zhou, Z., Fan, Z.-X., 2018. Growth response of *Abies georgei* to climate increases with elevation in the central Hengduan Mountains, southwestern China. Dendrochronologia 47, 1–9. https://doi.org/10.1016/j.dendro.2017.11.001.
Panthi, S., Fan, Z.-X., van der Sleen, P., Zuidema, P.A., 2020. Long-term physiological and growth responses of Himalayan fir to environmental change are mediated by mean climate. Glob. Chang. Biol. 26 (3), 1778–1794. https://doi.org/10.1111/gcb.14910.
R Core Team, 2020. R: a Language and Environment for Statistical Computing. R Foundation for Statistical Computing, Vienna, Austria. https://www.R-project.org/.
Ranjitkar, S., Luedeling, E., Shrestha, K.K., Guan, K., Xu, J., 2013. Flowering phenology of tree rhododendron along an elevation gradient in two sites in the Eastern Himalayas. Int. J. Biometeorol. 57 (2), 225–240. https://doi.org/10.1007/s00484-012-0548-4.
Rayback, S.A., Henry, G.H.R., Lini, A., 2012. Multiproxy reconstructions of climate for three sites in the Canadian High Arctic using *Cassiope tetragona*. Clim. Change 114, 593–619. https://doi.org/10.1007/s10584-012-0431-7/.
Rayback, S.A., Shrestha, K.B., Hofgaard, A., 2017. Growth variable-specific moisture and temperature limitations in cooccurring alpine tree and shrub species, central Himalayas, Nepal. Dendrochronologia 44, 193–202. https://doi.org/10.1016/j.dendro.2017.06.001.
Rinn, F., 2003. TSAP-Win User Reference Manual. Rinntech, Heidelberg, Germany.
Sabin, T.P., Krishnan, R., Vellore, R., Priya, P., Borgaonkar, H.P., Singh, B.P., Sagar, A., 2020. Climate change over the Himalayas. In: Raghavan, K., Jayanarayanan, S., Gnanaseelan, C., Mujumdar, M., Kulkarni, A., Chakraborty, S. (Eds.), Assessment of Climate Change Over the Indian Region, 1st ed. Springer, Singapore, pp. 207–222. https://doi.org/10.1007/978-981-15-4327-2_11.
Sano, M., Ramesh, R., Sheshshayee, M.S., Sukumar, R., 2012. Increasing aridity over the past 223 years in the Nepal Himalaya inferred from a tree-ring $\delta^{18}O$ chronology. Holocene 22 (7), 809–817. https://doi.org/10.1177/0959683611430338.
Schickhoff, U., Bobrowski, M., Bohner, J., Burzle, B., Chaudhary, R.P., Gerlitz, L., Wedegartner, R., 2014. Do Himalayan treelines respond to recent climate change? An evaluation of sensitivity indicators. Earth Syst. Dyn. 6 (1), 245–265. https://doi.org/10.5194/esd-6-245-2015.
Shah, S.K., Pandey, U., Mehrotra, N., Wiles, G.C., Chandra, R., 2019. A winter temperature reconstruction for the Lidder Valley, Kashmir, Northwest Himalaya based on tree-rings of *Pinus wallichiana*. Clim. Dyn. 53 (7), 4059–4075. https://doi.org/10.1007/s00382-019-04773-6.
Sigdel, S.R., Wang, Y., Camarero, J.J., Zhu, H., Liang, E., Penuelas, J., 2018. Moisture-mediated responsiveness of treeline shifts to global warming in the Himalayas. Glob. Chang. Biol. 24 (11), 5549–5559. https://doi.org/10.1111/gcb.14428.
Stokes, M.A., Smiley, T.L., 1996. An Introduction to Tree-Ring Dating. Arizona University Press, Chicago.
Tiwari, A., Fan, Z.-X., Jump, A.S., Zhou, Z.-K., 2017. Warming induced growth decline of Himalayan birch at its lower range edge in a semi-arid region of trans-Himalaya, central Nepal. Plant Ecol. 218 (5), 621–633. https://doi.org/10.1007/s11258-017-0716-z.
Trouet, V.M., Van Oldenborgh, G.J., 2013. KNMI climate explorer: a web-based research tool for high-resolution paleoclimatology. Tree-ring Res. 69 (1), 3–13. https://doi.org/10.3959/1536-1098-69.1.3.
Wang, T.M., Yang, S., Wen, Z.P., Wu, R.G., Zhao, P., 2011. Variations of the winter India-Burma Trough and their links to climate anomalies over southern and eastern Asia. J. Geophys. Res. 116, D23118 https://doi.org/10.1029/2011JD016373.
Ward, F.K., Bamsbottom, J., 1927. The Sino-Himalayan flora. Proc. Linn. Soc. London 139 (1), 67–74. https://doi.org/10.1111/j.1095-8312.1927.tb00074.x.
Wernicke, J., Stark, G., Grießinger, J., Wang, L., Bräuning, A., 2019. Air moisture signals in a stable oxygen isotope chronology of dwarf shrubs from the central Tibetan Plateau). Ann. Bot. 20, 1–12. https://doi.org/10.1093/aob/mcz030.
Wigley, T.M.L., Briffa, K.R., Jones, P.D., 1984. On the average value of correlated time series, with applications in dendroclimatology and hydrometeorology. J. Clim. Appl. Meteorol. 23 (2), 201–213. https://doi.org/10.1175/1520-0450(1984)023<0201:Otavoc>2.0.Co;2.
Williams, C.M., Henry, H.A., Sinclair, B.J., 2015. Cold truths: how winter drives responses of terrestrial organisms to climate change. Biol. Rev. 90 (1), 214–235. https://doi.org/10.1111/brv.12105.
Zang, C., Biondi, F., 2013. Dendroclimatic calibration in R: the boot res package for response and correlation function analysis. Dendrochronologia 31 (1), 68–74. https://doi.org/10.1016/j.dendro.2012.08.001.
Zang, C., Biondi, F., 2015. Treeclim: an R package for the numerical calibration of proxy-climate relationships. Ecography 38, 431–436. https://doi.org/10.1111/ecog.01335.
Zaw, Z., Fan, Z.-X., Bräuning, A., Xu, C., Liu, W.-J., Gaire, N.P., Panthi, S., Than, K.Z., 2020. Drought reconstruction over the past two centuries in southern Myanmar using teak tree-rings: linkages to the Pacific and Indian Oceans. Geophys. Res. Lett. 47 (10) https://doi.org/10.1029/2020GL087627 e 2020GL087627.
Zhang, R., Yuan, Y., Wei, W., Gou, X., Yu, S., Shang, H., Qin, L., 2015. Dendroclimatic reconstruction of autumn–winter mean minimum temperature in the eastern Tibetan Plateau since 1600 AD. Dendrochronologia 33, 1–7. https://doi.org/10.1016/j.dendro.2014.09.001.